Exploring the chemistry and photophysics of substitututed picolinates positional isomers in iridium(III)bisphenylpyridine complexes

Ross Davidson,* Yu-Ting Hsu, Chandni Bhagani, Dmitry Yufit, Andrew Beeby.*

Department of Chemistry, Durham University, South Rd, Durham, DH1 3LE, UK

KEYWORDS

Picolinate substitution, molecular building block, iridium, positional difference

ABSTRACT: A simple and versatile route for modifying picolinate ligands coordinated to iridium is described. Reacting a μ-chloro iridium(C^N) dimer (where C^N is a phenylpyridine based ligand) with bromopicolinic acid (HpicBr) yields the corresponding iridium(C^N)$_2$(picBr) complexes (**1**–**4** and **11**), which were readily modified by a Sonogashira reaction to give eight alkyne-substituted picolinate complexes (**5**–**10**, **12** and **13**). The luminescent behaviour of these complexes shows that the position of substitution about the picolinate ring has both an effect on photophysical behaviour as well as the reactivity.

Introduction

Complexes containing a Ir(C^N)$_2$(A) where (A = bidentate ancillary ligand) have frequently been employed in OLEDs because of their phosphorescence, quantum yield, emission tunablitiy and short lifetimes (typically 1–20 μs). Due to the modular nature of the complexes, it is possible to tune the energy of the excited state and emission by substituting the ligands in addition to controlling solubility etc.[1-8] These properties make them ideal for OLEDs but have also been used to sensitise the emission of another molecules. The most successful examples of this are the iridium–lanthanide complexes, in which the iridium complex is tethered to a lanthanide complex. By choosing ligands judiciously, it is possible to tune the T_1 energy of the iridium complex in such that it is sufficiently above the lanthanide D_0, allowing for a photo-induced energy transfer.[9-15] Such systems have been employed in bioimaging, in particular for in vivo $^1O_2$ sensing.[16, 17]

Depending on the nature of the tether between the iridium complexes and other molecules, energy transfers can occur via two different mechanisms: i) Förster energy transfers, which are common in unconjugated tethers but decay exponentially with distance

and rely on dipole-dipole coupling between transition dipole moments of the donor and acceptor;[18] and ii) Dexter energy transfers, which involve the electron exchange between donor and acceptor. tend to favour conjugated tethers, but which can occur over a 20 Å distance between the sensitizer and emitter.[19]

The most common approach to joining iridium sensitizers to an emitter is to attach the tether to the ancillary ligand of the iridium complex. This approach is favoured because the conditions required to coordinate the primary ligands are often harsh and lead to ligand exchange, but in contrast, the ancillary ligand coordinating conditions are typically mild, allowing for the ligand to be modified prior (or post) to coordination. The two most modified types of ancillary ligands are acetylacetonate (acac) and diimine ligands (e.g., 1,10-phenanthroline [phen] or 2,2ˈ-bipyridine [bpy]). Acetylacetonate has been extensively modified at the beta methyl (β-methyl) positions with an assortment of aromatic and alkyl groups;[20-26] the unoccupied orbitals of acac tend to be high in energy and therefore have little involvement in the photophysics of the complexes. Recently, however, Zeissel et al., by substituting the central position with aromatic groups containing accessible triplet states, have demonstrated that it is possible to introduce an interligand energy transfer.[26, 27] Diimine ligands tend to have low-lying π^* orbitals, which result in the iridium complexes' lowest unoccupied molecular orbitals (LUMOs) being strongly diimine in character. These have been tethered by a variety of groups including alkanes and napthylene to lanthanide complexes, to enhance their emission via either Förster or Dexter energy transfers.[9, 12, 28, 29]

Pyridine-2-carboxylate (*pic*) has been used extensively as a blue-shifting ancillary ligand in the production of OLED materials,[30-32] but surprisingly further elaboration of this ligand has largely been unexplored. One of the few examples that have been explored was 5-ethynylpicolinate attached to polyoxometalates (POMs), which demonstrated their potential for charge separation.[33-35] All other examples of *pic* modification have involved the addition

of electron-donating groups which raise the energy of the *pic* orbitals, thereby reducing their involvement in the frontier orbitals of the complex and properties of the excited state.[36-38] In the current investigation, we sought to examine the effects of substituting varied alkynes at different positions (Figure 1) around *pic* upon the photophysical properties of the complexes and establish which sites had the greatest effects in creating a pathway for the addition of other functional groups.

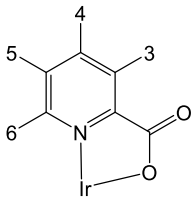

Figure 1. Pyridine-2-carboxylate positional labels.

Experimental Section

General details. NMR spectra were recorded in deuterated solvent solutions on a Varian VNMRS-600 spectrometer and were referenced against solvent resonances (^{1}H, ^{13}C). Electrospray mass spectra (ESMS) data were recorded on a TQD mass spectrometer (Waters Ltd, UK) in acetonitrile or MALDI TOF MS data were recorded on a Bruker Autoflex II ToF/ToF. Microanalyses were performed by Elemental Analysis Service, London Metropolitan University, UK. Electrochemical analyses of the complexes were carried out using a PalmSens EmStat^{2} potentiometer, with platinum working, platinum counter and platinum pseudo reference electrodes, from solutions in acetonitrile containing 0.1 M supporting electrolyte (tetrabutylammonium hexafluorophosphate [$TBAPF_6$]), with a scan rate of 100 mVs^{-1}. The ferrocene/ferrocinium couple was used as the internal reference. Analytical grades of solvents were used: $[Ir(PPy)_2Cl]_2$[43] and ((4-ethynylphenyl)ethynyl)triisopropylsilane[44] were synthesised according to literature methods. All other chemicals were sourced from standard suppliers.

Synthesis of Ir(ppy)$_2$(pic-X-Br) complexes. $[(ppy)_2IrCl]_2$ (0.50 g, 0.46 mmol), bromopicolinic acid (0.28 g, 1.38 mmol), and K_2CO_3 (0.38 g, 2.76 mmol) were dissolved in

anhydrous acetone (30 mL), and the solution was heated to reflux overnight under nitrogen. The solvent was removed *in vacuo*, leaving a yellow solid, which was dissolved in dichloromethane (DCM) and filtered. The yellow filtrate was purified by column chromatography on silica, eluted using a gradient from dichloromethane to acetone, yielding a yellow-orange solid. Crystals were grown by layer diffusion of methanol into a dichloromethane solution.

Ir(ppy)$_2$(pic-3-Br) 1. Yield: 0.52 g (80 %). ^{1}H-NMR (CD_2Cl_2) δ 8.70 (dd (J_{HH} = 6, 1 Hz), 1H), 8.14 (dd (J_{HH} = 8, 1 Hz), 1H), 7.95 (dt (J_{HH} = 8, 1 Hz), 1H), 7.89 (dt (J_{HH} = 8, 1 Hz), 1H), 7.83 (dd (J_{HH} = 8, 1 Hz), 1H), 7.80-7.75 (m, 2H), 7.66 (dd (J_{HH} = 6, 1 Hz), 2H), 7.54 (dd (J_{HH} = 6, 2 Hz), 1H), 7.19 (ddd (J_{HH} = 7, 6, 1), 1H), 7.12 (dd (J_{HH} = 8, 5 Hz), 1H), 7.02 (ddd (J_{HH} = 7, 5, 1 Hz), 1H), 6.97-6.91 (m, 2H), 6.82-6.77 (m, 2H), 6.36 (dd (J_{HH} = 8, 1 Hz), 1H), 6.16 (dd (J_{HH} = 8, 1 Hz), 1H) ppm. ^{13}C-NMR (CD_2Cl_2) δ: 169.9, 168.4, 167.4, 148.6, 148.5, 148.4, 147.6, 144.5, 144.2, 137.4, 137.3, 132.3, 132.2, 129.8, 129.4, 127.7, 125.0, 124.5, 124.1, 122.4, 121.5, 121.1, 119.2, 118.7 ppm. MALDI: m/z 701.0 $[M]^+$. Anal. Calc. for $C_{28}H_{19}BrIrN_3O_2$: C, 47.93; H, 2.73; N, 5.99 %. Found: C, 47.86; H, 2.79; N, 6.05 %.

Ir(ppy)$_2$(pic-4-Br) 2. Yield: 0.56 g (87%). ^{1}H-NMR (CD_2Cl_2) δ 8.69 (d (J_{HH} = 6 Hz), 1H), 8.44 (d (J_{HH} = 2 Hz), 1H), 7.96 (d (J_{HH} = 8 Hz), 1H), 7.90 (d (J_{HH} = 8 Hz), 1H), 7.81-7.75 (m, 2H), 7.67 (m, 2H), 7.59 (d (J_{HH} = 6 Hz), 1H), 7.56 (d (J_{HH} = 6 Hz), 1H), 7.50 (dd (J_{HH} = 6 , 2 Hz),1H), 7.18 (td (J_{HH} = 7, 2 Hz), 1H), 7.03 (td (J_{HH} = 7, 2 Hz), 1H), 6.96 (m, 2H), 6.81 (m, 2H), 6.39 (d (J_{HH} = 8 Hz), 1H), 6.20 (d (J_{HH} = 8 Hz), 1H) ppm. ^{13}C-NMR (CD_2Cl_2) δ: 171.0, 168.5, 167.4, 153.3, 148.9, 148.8, 148.7, 148.2, 146.5, 144.3, 144.2, 137.5, 137.4, 134.8, 132.2, 131.7, 131.4, 129.9, 129.5, 124.5, 124.1, 122.4, 121.7, 121.3, 119.2, 118.7. ESMS: m/z 702.0359 $[M+H]^+$. Anal. Calc. for $C_{28}H_{19}BrIrN_3O_2$: C, 47.93; H, 2.73; N, 5.99 %. Found: C, 48.02; H, 2.73; N, 6.06 %.

Ir(ppy)$_2$(pic-5-Br) 3. Yield: 0.34 g (53 %). ^{1}H-NMR-(CD_2Cl_2) δ: 8.67 (s, 1H), 8.15 (d (J_{HH} = 8 Hz), 1H), 8.04 (d (J_{HH} = 8 Hz), 1H), 7.95 (d (J_{HH} = 8 Hz), 1H), 7.90 (d (J_{HH} = 8

Hz), 1H), 7.79-7.76 (m, 3H), 7.68-7.65 (m, 2H), 7.55 (d (J_{HH} = 6 Hz), 1H), 7.18 (t (J_{HH} = 8 Hz), 1H), 7.02 (t (J_{HH} = 8 Hz), 1H), 6.98 (t (J_{HH} = 8 Hz), 1H), 6.93 (t (J_{HH} = 8 Hz), 1H), 6.81 (t (J_{HH} = 8 Hz), 1H), 6.37 (d (J_{HH} = 7 Hz), 1H), 6.15 (d (J_{HH} = 7 Hz) ppm. ^{13}C-NMR (CD_2Cl_2) δ: 171.4, 168.4, 167.4, 151.1, 149.2, 148.6, 148.4, 148.2, 146.2, 144.2, 144.1, 140.5, 137.4, 137.4, 132.3, 132.1, 129.9, 129.4, 129.1, 124.8, 124.5, 124.0, 122.4, 122.4, 121.3, 119.1, 118.8 ppm. MALDI: m/z 701.0 $[M]^+$. Anal. Calc. for $C_{28}H_{19}BrIrN_3O_2$: C, 47.93; H, 2.73; N, 5.99 %. Found: C, 47.91; H, 2.89; N, 6.06 %.

Ir(ppy)$_2$(pic-6-Br) 4. Yield: 0.55 g (85 %). ^{1}H-NMR (CD_2Cl_2) δ: 8.59 (dt (J_{HH} = 6, 1 Hz), 1H), 8.35 (dd (J_{HH} = 8, 1 Hz), 1H), 7.95-7.89 (m, 3H), 7.81-7.76 (m, 3H), 7.64-7.60 (m, 3H), 7.14 (ddd (J_{HH} = 7, 6, 1 Hz), 1H), 7.05 (ddd (J_{HH} = 7, 6, 1 Hz), 1H), 6.92 (td (J_{HH} = 8, 1 Hz), 1H), 6.85 (td (J_{HH} = 8, 1 Hz), 1H), 6.74 (td (J_{HH} = 7, 2 Hz), 1H), 6.68 (td (J_{HH} = 7, 2 Hz), 1H), 6.31 (dd (J_{HH} = 8, 1 Hz), 1H), 6.00 (dd (J_{HH} = 8, 1 Hz), 1H) ppm. ^{13}C-NMR (CD_2Cl_2) δ: 172.0, 168.6, 167.6, 155.5, 150.4, 149.5, 147.9, 145.0, 143.9, 143.8, 143.8, 139.5, 137.3, 137.3, 133.3, 133.1, 131.3, 129.3, 129.0, 127.0, 124.0, 123.9, 122.6, 121.8, 121.6, 120.4, 119.2, 118.5 ppm. MALDI: m/z 701.0 $[M]^+$. Anal. Calc. for $C_{28}H_{19}BrIrN_3O_2$: C, 47.93; H, 2.73; N, 5.99 %. Found: C, 47.91; H, 2.82; N, 5.90 %.

Triisopropylsilyl acetylene coupling procedure. In a nitrogen-degassed atmosphere, Ir(ppy)$_2$(pic-X-Br) (0.10 g, 0.14 mmol), CuI (0.003 g, 0.014 mmol), and [Pd(PPh$_3$)$_2$Cl$_2$] (0.01 g, 0.014 mmol) were dissolved in anhydrous tetrahydrofuran (THF) (20 mL) before triethylamine (NEt$_3$, 7 mL) was added. After three freeze-pump-thaw cycles, triisopropylsilyl acetylene (Tips-CCH, 0.1 mL, 0.446 mmol) was added, and the solution was heated overnight at 50°C. The reaction mixture was evaporated to dryness, and the product was isolated and purified using column chromatography on silica gel, using a solvent gradient from DCM to acetone to afford an orange-red solid.

Ir(ppy)$_2$(pic-3-C≡C-Tips) 5. Yield: 0.55 g (85 %). ^{1}H-NMR (CD_2Cl_2) δ 8.75 (d (J_{HH} = 6 Hz), 1H), 7.99 (d (J_{HH} = 8 Hz), 1H), 7.93 (d (J_{HH} = 8 Hz), 1H), 7.88 (d (J_{HH} = 8 Hz), 1H), 7.78-7.72 (m, 3H), 7.65 (d (J_{HH} = 8 Hz), 2H), 7.53 (d (J_{HH} = 6 Hz), 1H), 7.22 (t (J_{HH} = 6 Hz),

1H), 7.18 (t (J_{HH} = 6 Hz), 1H), 7.01 (t (J_{HH} = 6 Hz), 1H), 6.96-6.92 (m, 2H), 6.82-6.77 (m, 2H), 6.37 (d (J_{HH} = 8 Hz), 1H), 6.17 (d, (J_{HH} = 8 Hz), 1H), 1.18 (pseudo s, 21H) ppm. ^{13}C-NMR (CD_2Cl_2) δ: 170.5, 168.4, 167.4, 152.2, 149.2, 148.8, 148.2, 147.9, 147.7, 144.3, 144.2, 137.3, 137.2, 132.3, 132.2, 129.8, 129.3, 126.6, 124.8, 124.4, 124.0, 122.4, 121.4, 121.0, 119.1, 118.6, 103.2, 102.3, 18.4, 11.3 ppm. MALDI: m/z 803.2 $[M]^+$. Anal. Calc. for $C_{39}H_{40}IrN_3O_2Si \cdot CH_2Cl_2$: C, 54.10; H, 4.77; N, 4.73 %. Found: C, 54.52; H, 4.75; N, 4.91 %.

Ir(ppy)$_2$(pic-4-C≡C-Tips) 6. Crystals were grown by layer diffusion of methanol into a dichloromethane solution. Yield: 0.10 g (90 %). ^{1}H-NMR (CD_2Cl_2) δ: 8.69 (d (J_{HH} = 6 Hz), 1H), 8.27 (d (J_{HH} = 2 Hz), 1H), 7.96 (d (J_{HH} = 8 Hz), 1H), 7.90 (d (J_{HH} = 8 Hz), 1H), 7.78 (m, 2H), 7.71 (d (J_{HH} = 6 Hz), 1H), 7.67 (m, 2H), 7.56 (d (J_{HH} = 6 Hz), 1H), 7.32 (dd (J_{HH} = 6, 2), 1H), 7.18 (td (J_{HH} = 7, 2 Hz), 1H), 7.03 (td (J_{HH} = 7, 2 Hz), 1H), 6.96 (m, 2H), 6.81 (m, 2H), 6.39 (d (J_{HH} = 8 Hz), 1H), 6.20 (d (J_{HH} = 8 Hz), 1H), 1.13 (pseudo s, 21H) ppm. ^{13}C-NMR (CD_2Cl_2) δ 171.8, 168.6, 167.4, 152.1, 149.5, 148.6, 148.2, 148.1, 146.9, 144.3, 144.2, 137.4, 137.3, 133.0, 132.3, 132.2, 130.4, 130.0, 129.8, 129.4, 124.4, 124.1, 122.4, 122.3, 121.6, 121.1, 119.2, 118.7, 102.9, 101.1, 18.3, 11.1 ppm. ESMS: m/z 804.2634 $[M+H]^+$. Anal. Calc. for $C_{39}H_{40}IrN_3O_2Si$: C, 58.33; H, 5.02; N, 5.23 %. Found: C, 58.24; H, 5.12; N, 5.19 %.

Ir(ppy)$_2$(pic-5-C≡C-Tips)$_2$ 7. Crystals were grown by layer diffusion of methanol into a dichloromethane solution. Yield: 0.058 g (51 %). ^{1}H-NMR (CD_2Cl_2) δ: 8.70 (dt (J_{HH} = 6, 1 Hz), 1H), 8.21 (dd (J_{HH} = 8, 1 Hz), 2H), 7.95-7.89 (m, 3H), 7.79-7.74 (m, 3H), 7.67 (ddd (J_{HH} = 8, 4, 1 Hz), 2H), 7.58 (d (J_{HH} = 6 Hz), 1H), 7.17 (ddd (J_{HH} = 7, 6, 1 Hz), 1H), 7.00 (ddd (J_{HH} = 7, 6, 1 Hz), 1H), 6.98-6.93 (m, 2H), 6.84-6.80 (m, 2H), 6.41 (dd (J_{HH} = 8, 1 Hz), 1H), 6.22 (dd (J_{HH} = 8, 1 Hz), 1H), 1.07 (pseudo s, 21H) ppm. ^{13}C-NMR (CD_2Cl_2) δ: 171.8, 168.4, 167.5, 151.1, 150.8, 149.0, 148.6, 148.3, 146.5, 144.3, 144.1, 139.9, 137.4, 137.3, 132.3, 132.2, 129.8, 129.4, 127.4, 124.8, 124.4, 124.1, 122.4, 122.3, 121.5, 121.3, 119.1, 118.8, 101.4, 99.5, 18.2, 11.0 ppm. MALDI: m/z 803.2 $[M]^+$. Anal. Calc. for $C_{39}H_{40}IrN_3O_2Si$: C, 58.33; H, 5.02; N, 5.23 %. Found: C, 58.22; H, 5.21; N, 5.19 %.

$Ir(ppy)_2$(pic-6-C≡C-Tips) 8. Crystals were grown by evapouration of a benzene solution. Yield: 0.051 g (45 %). ^{1}H-NMR (CD_2Cl_2) δ: 8.52 (dd (J_{HH} = 6, 2 Hz), 1H), 8.27 (dd (J_{HH} = 8, 2 Hz), 1H), 8.11 (dd (J_{HH} = 6, 2 Hz), 1H), 7.93 (dt (J_{HH} = 8, 1 Hz), 1H), 7.86-7.83 (m, 2H), 7.79 (td (J_{HH} = 8, 2 Hz), 1H), 7.71 (td (J_{HH} = 8, 2 Hz), 1H), 7.61 (dd (J_{HH} = 8, 1 Hz), 2H), 7.56 (dd (J_{HH} = 8, 1 Hz), 1H), 7.10 (td (J_{HH} = 8, 1 Hz), 1H), 7.03 (td (J_{HH} = 8, 1 Hz), 1H), 6.90 (td (J_{HH} = 8, 1 Hz), 1H), 6.80 (td (J_{HH} = 8, 1 Hz), 1H), 6.72 (td (J_{HH} = 8, 1 Hz), 1H), 6.63 (td (J_{HH} = 8, 1 Hz), 1H), 6.33 (dd (J_{HH} = 8, 1 Hz), 1H), 5.98 (dd (J_{HH} = 8, 1 Hz), 1H), 0.99-0.95 (m, 21H) ppm. ^{13}C-NMR (CD_2Cl_2) δ: 172.4, 168.6, 167.9, 153.3, 149.8, 149.2, 147.5, 146.4, 144.9, 143.9, 143.5, 137.3, 1371, 137.0, 135.4, 133.0, 131.5, 129.4, 1292, 127.2, 124.0, 123.8, 122.4, 121.6, 121.4, 119.1, 118.2, 105.6, 103.6, 18.6, 11.5 ppm. MALDI: m/z 803.3 $[M]^+$. Anal. Calc. for $C_{39}H_{40}IrN_3O_2Si·½CH_2Cl_2$: C, 56.11; H, 4.89; N, 4.97 %. Found: C, 56.04; H, 4.63; N, 4.50 %.

Coupling procedure for HC≡C-C_6H_4-C≡C-Tips. In a nitrogen-degassed atmosphere, $Ir(ppy)_2$(pic-X-Br) (0.20 g, 0.285 mmol), CuI (0.006 g, 0.029 mmol), $[Pd(PPh_3)_2Cl_2]$ (0.02 g, 0.029 mmol), and HC≡C-C_6H_4-C≡C-Tips (0.097 g, 0.343 mmol) were dissolved in anhydrous THF (30 mL). After three freeze-pump-thaw cycles, NEt_3 (7 mL) was added, and the solution was heated to 50°C for 12 hours. The reaction mixture was evaporated to dryness, and the product was isolated and purified using column chromatography on silica eluted by a gradient of DCM to acetone to afford an orange solid.

$Ir(ppy)_2$(pic-4-C≡C-C_6H_4-C≡C-Tips) 9. Crystals were grown by layer diffusion of methanol into a dichloromethane solution. Yield: 0.22 g (87%). ^{1}H-NMR (CD_2Cl_2) δ: 8.71 (d (J_{HH} = 6 Hz), 1H), 8.33 (d (J_{HH} = 2 Hz), 1H), 7.95 (d (J_{HH} = 8 Hz), 1H), 7.89 (d (J_{HH} = 8 Hz), 1H), 7.75-7.68 (m, 3H), 7.67 (d (J_{HH} = 8 Hz), 2H), 7.57 (d (J_{HH} = 6 Hz), 1H) 7.56-7.44 (m, 4H), 7.38 (dd (J_{HH} = 6, 2 Hz), 1H), 7.18 (ddd (J_{HH} = 7, 6, 1 Hz), 1H), 7.01 (ddd (J_{HH} = 7, 6, 1 Hz), 1H), 6.96 (*t* (J_{HH} = 7 Hz), 1H), 6.89 (t (J_{HH} = 7 Hz), 1H), 6.84 (t (J_{HH} = 7 Hz), 1H), 6.79 (t (J_{HH} = 7 Hz), 1H), 6.40 (d (J_{HH} = 8 Hz), 1H), 6.20 (d (J_{HH} = 8 Hz), 1H), 1.15 (pseudo s, 21H) ppm. ^{13}C-NMR (CD_2Cl_2) δ: 171.8, 168.6, 167.4, 152.2, 149.5, 148.7, 148.2, 146.9, 144.3, 144.2, 137.4, 137.3, 132.8, 132.3, 132.0, 131.9, 130.0, 129.8, 129.4, 129.4, 124.9, 124.4, 124.1, 122.4, 122.3, 121.6, 121.2, 121.1, 119.2, 118.7, 106.1, 96.5, 94.1, 87.6, 18.4, 11.3. ESMS: m/z 904.2953 $[M+H]^+$. Anal. Calc. for $C_{47}H_{44}IrN_3O_2Si$: C, 62.50; H, 4.91; N, 4.65 %. Found: C, 62.57; H, 4.97; N, 4.55 %.

$Ir(ppy)_2$(pic-5-C≡C-C_6H_4-C≡C-Tips) 10. Yield: 0.11 g (45 %). ^{1}H-NMR (CD_3CN) δ: 8.62 (dd (J_{HH} = 6, 1 Hz), 1H), 8.17 (d (J_{HH} = 8 Hz), 1H), 8.10 (dd, (J_{HH} = 8, 2 Hz), 1H), 8.06 (d (J_{HH} = 8 Hz), 1H), 8.03 (d (J_{HH} = 8 Hz, 1H), 7.90-7.89 (m, 2H), 7.80 (d (J_{HH} = 2 Hz), 1H), 7.76-7.72 (m, 3H), 7.48-7.44 (m, 4H), 7.27 (td (J_{HH} = 7, 1 Hz), 1H), 7.12 (td (J_{HH} = 7,1 Hz), 1H), 6.96 (td (J = 7, 1 Hz), 1H), 6.91 (td (J = 7, 1 Hz), 1H), 6.83 (td (J = 7, 1 Hz), 1H), 6.77 (td (J_{HH} = 7, 1 Hz), 1H), 6.37 (d (J_{HH} = 7 Hz), 1H), 6.14 (d, (J_{HH} = 7 Hz), 1H), 1.18-1.10 (m, 21H) ppm. ^{13}C-NMR (CD_2Cl_2) δ: 171.8, 168.4, 167.5, 150.9, 150.4, 148.8, 148.6, 148.2, 146.6, 144.3, 144.1, 140.1, 137.4, 137.3, 132.3, 132.2, 131.9, 131.5, 129.9, 129.4, 127.6, 124.6, 124.5, 124.0, 122.4, 122.3, 121.6, 121.2, 119.1, 118.8, 106.1, 95.2, 93.9, 85.84, 18.3, 11.2 ppm. MALDI: m/z 903.2 $[M]^+$. Anal. Calc. for $C_{47}H_{44}IrN_3O_2Si{\cdot}2CH_3O$: C, 60.85; H, 5.42; N, 4.34 %. Found: C, 60.72; H, 5.32; N, 4.48 %.

$Ir(Phppy)_2$(pic-4-Br) (11). 2,4-diphenylpyridine (Phppy, 1.00 g, 4.32 mmol) and $IrCl_3{\cdot}3H_2O$ (506 mg, 1.44 mmol) were added to a solution of 2-ethoxyethanol:water (30 mL, 1:1) and heated to 110°C for 8 hours. The solution was cooled to room temperature and poured into water (100 mL). The orange precipitate was collected by filtration, dissolved in DCM, dried over $MgSO_4$, and passed through a silica plug eluted by DCM; the solvent was removed. The solid was subsequently added to a suspension containing 4-bromopicolinic acid (872 mg, 4.32 mmol) and K_2CO_3 (596 mg, 4.32 mmol) in acetone (50 mL). The suspension was heated to 50°C for 12 hours before the solvent was removed, dissolved in DCM, and filtered. The filtrate was purified via silica chromatography eluted by acetone, and the emissive fraction was collected; the solvent was then removed to yield the product. Crystals were grown by evaporation of a DCM and MeOH solution. Yield: 601 mg (49 %). ^{1}H-NMR (CD_2Cl_2) δ: 8.72 (d (J_{HH} = 6 Hz), 2H), 8.46 (d (J_{HH} = 2 Hz), 1H), 8.16 (d (J_{HH} = 2 Hz), 1H), 8.11 (d (J_{HH} = 2 Hz), 1H), 7.79-7.77 (m, 6H), 7.64 (d (J_{HH} = 6 Hz), 1H), 7.61 (d (J_{HH} = 6 Hz), 1H), 7.58-7.55 (m, 4H), 7.53-7.50 (m, 3H), 7.42 (dd (J_{HH} = 6, 2 Hz), 1H), 7.26 (dd (J_{HH} = 6, 2 Hz), 1H), 7.01-6.96 (m, 2H), 6.87-6.82 (m, 2H), 6.52 (d (J_{HH} = 8 Hz), 1H), 6.33 (d (J_{HH} = 8 Hz), 1H) ppm. ^{13}C-NMR (CD_2Cl_2) δ: 171.0, 168.6, 167.4, 153.3, 149.9, 149.7, 149.1, 148.9, 148.6, 148.2, 146.7, 144.3, 144.1, 137.1, 137.0, 134.8, 132.4, 131.6, 131.4, 129.9, 129.7, 129.5, 129.1, 127.1, 124.4, 124.1, 121.6, 121.2, 120.6, 120.5, 116.9, 116.3 ppm. MALDI: m/z 853.0 $[M]^+$. Anal. Calc. for $C_{40}H_{27}BrIrN_3O_2{\cdot}CH_2Cl_2$: C, 52.46; H, 3.11; N, 4.48 %. Found: C, 52.28; H, 3.12; N, 4.42 %.

Ir(Phppy)$_2$(pic-4-C≡C-Tips) (12). The same procedure as previously described for complexes **5–8** except **11** was used in place of Ir(ppy)$_2$(pic-X-Br) to yield an orange solid. Crystals were grown by evaporation of a DCM and MeOH solution. Yield: 123 mg (92 %). ^{1}H-NMR (CD_2Cl_2) δ: 8.74 (d (J_{HH} = 6 Hz), 1H), 8.31 (d (J_{HH} = 2 Hz), 1H), 8.17 (d (J_{HH} = 2 Hz), 1H), 7.80-7.78 (m, 7H), 7.63 (d (J_{HH} = 6 Hz), 1H), 7.58-7.56 (m, 4H), 7.53-7.50 (m, 3H), 7.42 (dd (J_{HH} = 6, 2 Hz), 1H), 7.35 (J_{HH} = 6, 2 Hz), 1H), 7.25 (dd (J_{HH} = 6, 2 Hz), 1H), 7.02-6.97 (m, 2H), 6.86-6.84 (m, 2H), 6.53 (dd (J_{HH} = 8, 1 Hz), 1H), 6.36 (dd (J_{HH} = 8, 1 Hz), 1H), 1.14 (pseudo s, 21H) ppm. ^{13}C-NMR (CD_2Cl_2) δ: 171.9, 168.6, 167.5, 152.1, 149.8, 149.6, 148.6, 148.3, 148.2, 147.0, 144.3, 144.1, 137.2, 137.1, 133.0, 132.5, 130.4, 130.0, 129.8, 129.7, 129.5, 129.1, 127.1, 124.4, 124.1, 121.6, 121.2, 120.6, 120.4, 116.9, 116.3, 102.9, 101.1, 18.3, 11.1 ppm. MALDI: m/z 955.3 $[M]^+$. Anal. Calc. for $C_{51}H_{48}IrN_3O_2Si{\cdot}CH_2Cl_2$: C, 60.04; H, 4.84; N, 4.04 %. Found: C, 59.95; H, 4.79; N, 3.99 %.

Ir(Phppy)$_2$(pic-4-C≡C-C$_6$H$_4$-C≡C-Tips) (13) The same procedure as previously described for complexes **9** and **10** except **11** was used in place of Ir(ppy)$_2$(pic-X-Br) to yield an orange solid. Yield: 131 mg (89 %). ^{1}H-NMR ($CDCl_3$) δ: 8.82 (d (J = 6 Hz), 1H), 8.40 (s, 1H), 8.08 (s, 1H), 8.04 (s, 1H), 7.78 (d (J_{HH} = 6 Hz), 1H), 7.75-7.68 (m, 5H), 7.56-7.44 (m, 12H), 7.36-7.34 (m, 2H), 7.15 (dd (J_{HH} = 6, 2), 1H), 6.97 (t (J_{HH} = 8 Hz), 1H), 6.89 (t (J_{HH} = 8 Hz), 1H), 6.85 (t (J_{HH} = 8 Hz), 1H), 6.79 (t (J_{HH} = 8 Hz), 1H), 6.54 (dd (J_{HH} = 8, 1 Hz), 1H), 6.31 (d (J_{HH} = 8 Hz), 1H), 1.13 (pseudo s, 21H) ppm. ^{13}C-NMR ($CDCl_3$) δ: 169.2, 167.6, 149.7, 149.6, 149.2, 148.9, 148.0, 147.2, 144.1, 144.0, 137.3, 137.1, 132.9, 132.7, 132.6, 132.1, 131.8, 130.3, 130.0, 129.7, 129.6, 129.4, 129.2, 127.1, 125.0, 124.3, 124.0, 121.6, 121.1, 120.3, 120.2, 116.8, 116.1, 106.1, 97.0, 94.1, 87.6, 18.6, 11.2 ppm. MALDI: m/z 1055.5 $[M]^+$. Anal. Calc. for $C_{59}H_{52}IrN_3O_2Si$: C, 67.15; H, 4.97; N, 3.98 %. Found: C, 66.89; H, 4.79; N, 3.89 %.

Crystallography

The single crystal X-ray data for all compounds were collected at 120.0(2) K on a Bruker D8Venture 3-circle diffractometer (Photon100 CMOS detector, IμS microsource, focusing mirrors, λMoKα, λ = 0.71073 Å) equipped with Cryostream (Oxford Cryosystems) open-flow nitrogen cryostat. Following multi-scan absorption corrections and solution by direct methods, the structures were refined against F^2 with full-matrix least-squares using the SHELXTL[45] and OLEX2[46] software. Anisotropic displacement parameters were employed for the non-disordered non-hydrogen atoms. The crystallographic and refinement parameters are listed in supporting information. Crystallographic data for the structures have been deposited with the Cambridge Crystallographic Data Centre as supplementary publication CCDC-1533394-1533402.

Computational. Density functional theory (DFT) calculations were carried out using the Gaussian 09 package (Gaussian, Inc)[47], all results were displayed using GaussView[48] and GaussSum[49]. All calculations used the B3LYP level set employing two different basis sets, SDD and 6-31G(d)/LANL2DZ, geometrically optimised in a DCM solvent field using the SCRF-PCM method. As a means of validating the computational models the structural accuracy were compared to with the experimental data by measuring the mean average deviation (MAD) values of the X-ray crystallography and vibrational data shown in Tables S4.1, finding SDD to be the best suited for these complexes.

RESULTS AND DISCUSSION

Synthesis. In our initial strategy to synthesise alkynyl-substituted picolinate $Ir(ppy)_2$(*pic*)-based complexes, we attempted to prepare the picolinic acid derivatives prior to complexation and to prevent the sequestration of the catalyst by the respective picolinic acid these complexes were attempted with the corresponding ethyl-ester. However, it was found that under the Sonogashira conditions required for coupling (typically including heating to

60-80°C) the bromo substituted ethylpicolinate became unstable. Although ^{1}H NMR and mass-spectrometry indicated that the desired product was the major species, many additional species were formed that proved difficult to separate. To avoid this problem, the bromo-substituted picolinic acid (H*pic*-Br) was coordinated to the $Ir(ppy)_2$ or $Ir(Phppy)_2$ first, to yield the respective bromo-substituted $Ir(ppy)_2$(pic-Br) complexes **1**, **2**, **3**, **4** and **12,** and these reacted further with a range of reagents (see Scheme 1). It was necessary to perform the reaction of the H*pic*-Br with the $[Ir(ppy)_2Cl]_2$ in an aprotic solvent (acetone) to prevent solvolysis of the bromide. The yields of complexes **1**, **2** and **4** ranged from 80% to 87%, while the limited solubility of complexes **3** and **11** greatly reduced the yield to 53% and 49% respectively, largely because the low solubility of the complex made purification difficult. As a means of assessing the reactivity of the metallo-synthons, complexes **1**, **2**, **3**, **4** and **11** were reacted under Sonogashira conditions ($PdCl_2(PPh_3)_2$, CuI, Et_3N, THF, 70°C) with either triisopropylsilyl acetylene (HC≡C-Tips) to give complexes **5**, **6**, **7**, **8** and **12** respectively or with (4-ethynylphenyl)ethynyl)triispropylsilane (HC≡C-C_6H_4-C≡C-Tips) to give complexes **9**, **10** and **13** respectively. The reaction between complex **2** and HC≡C-Tips to give complex **6** was fast, rapidly proceeding to completion in under six hours at only 50°C and gave a yield of 90%. The reaction with complex **1** (to give complex **5**) required a higher temperature but still gave an 85% yield. When complex **3** (to give complex **7**) was used, the yield dropped significantly to 51%, mainly owing to the insolubility of complex **3** even when heated. Finally, the reaction of complex **4** with HC≡C-Tips (to form complex **8**) gave a yield of only 35%, however, this reflects the difficulty in purifying the complex: unlike the other complexes, this compound could not be purified by chromatography because of its instability on silica, therefore it was necessary to purify the complex by fractional recrystallization. As expected the use of 2,4-diphenylpyridine in place of 2-phenylpyridine for complex **11** had no

impact on the reactivity of the complex with HC≡C-Tips (to give complex **12**), and had the advantage that the improved solubility allowed for a more efficient purification.

The positional difference in reactivity of the complexes became even more pronounced when HC≡C-C_6H_4-C≡C-Tips was reacted with complexes **2**, **3** and **11** the alkyne substituted complexes **9** (87% yield), **10** (45% yield) and **13** (89% yield) were formed in a similar fashion to the -C≡C-Tips analogues. However, when complex **1** or **4** was used, no product was observed. The limited reactivity of complex **4** could be attributed to the combination of steric hindrance about the bromo-reactive site and the increased size and rigidity of HC≡C-C_6H_4-C≡C-Tips compared to HC≡C-Tips. The proposed reason for the absence of product when reacting with complex **1** could be attributed to the formation of an intermediate species in which a $PdCl_2$ fragment coordinated to both the carbonyl group of the pic and ortho alkyne, destabilising the complex, though not isolated. The major species detected by MALDI at m/z 921.6 corresponds to the Tips deprotected complex coordinated to $PdCl_2$. Bian and Huang demonstrated that such coordination behaviour is possible where a pic substituted with an ortho phenol was able to coordinate a BF_2 fragment and lanthanides(III) ions.[11, 39, 40] In the shorter analogous complex **5** had the Tips group act to sterically hinder the alkyne effectively preventing efficient coordination to the Pd(II) ion.

This research demonstrates that for the bromopicolinates the 4-position of the pyridine is the most reactive, while complexes **3**, **5** and **6** had lower reactivity. In these examples, complexes substituted at the 5-position complexes had lower solubility. In an attempt to further extend the length of the ethynyl-phenylene groups 1-(tert-butyl)-4-((4-ethynylphenyl)ethynyl), benzene was reacted with complex **2**. However, the material formed proved to be insoluble in all available solvents, preventing purification and characterisation; therefore, we could only speculate that the desired product had been formed but the increased length had significantly reduced the complexes solubility. This would indicate that should the length of these

complexes be further extended, they would require additional solubilising groups, possibly on the 2-phenylpyridine ligands.

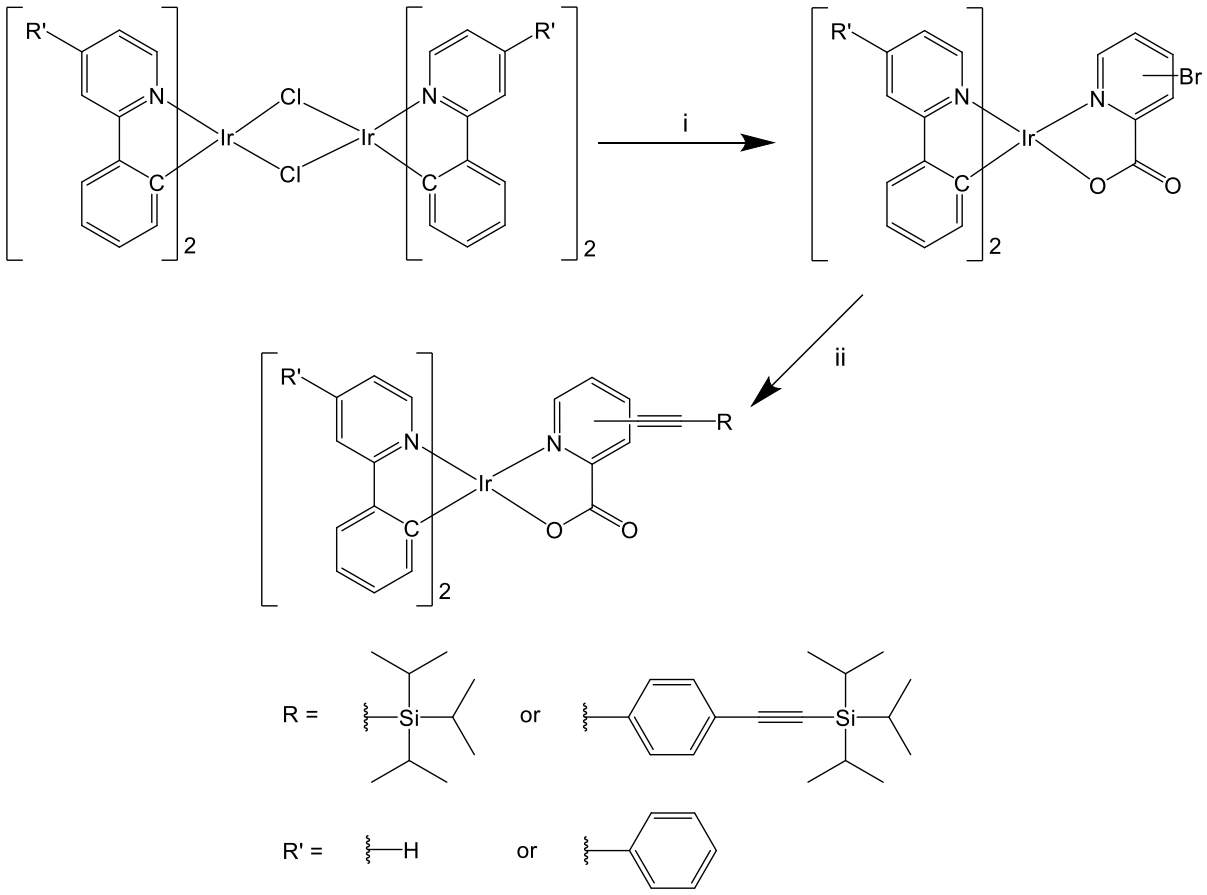

Scheme 1. Schematic synthesis of complexes **1**–**13**: i) Acetone, K_2CO_3, and 3-bromopicolinic acid, R' = H (**1**); 4-bromopicolinic acid, R' = H (**2**); 5-bromopicolinc acid, R' = H (**3**); 6-bromopicolinic acid, R' = H (**4**) or 4-bromopicolinic acid, R' = Ph (**11**); ii) THF, Et_3N, $Pd(PPh_3)_2Cl_2$ and triisopropylsilylacetylene {**5** (position 3), **6** (position 4), **7** (position 5), **8** (position 6) or **12** (position 4)} or ((4-ethynylphenyl)ethynyl)triispropylsilane {**9** (position 4), **10** (position 5) or **13** (position 4)}.

Molecular Structures.

The composition of the complexes **2-6**, **8, 10-12** have been confirmed by single-crystal X-ray crystallography. The details of the SXRD experiments are given in SI, the CCDC numbers for

structures are 1533394-1533402. In all determined structures Ir-atoms adopt usual and expected slightly distorted octahedral coordination. Planar ppy moieties are mutually perpendicular and its nitrogen atoms are located in opposite vertices of the coordination octahedron, typical of iridium complexes containing an $Ir(ppy)_2$ fragment. The geometrical parameters of the complexes are close to the values reported for $Ir(PPy)_2$(*pic*),[32] however, in the case of 6-substituted Pic complexes **4** and **8** steric repulsion between the 6-substitutent and one of the ppy groups results in slight distortion of the coordination octahedrons: the corresponding N(*pic*)-Ir-C(ppy) angles are increased to 104.01(6) and 105.2(2)°·respectively.

The average value of analogous angles in other studied compounds is 97.1°. The described complexes show a wide variety of different intermolecular interactions in crystals, mainly the C-H…O and C-H…Hal (Br, Cl) weak hydrogen bonds, but only in the structure **12** was a direct π…π interaction between ppy systems found.

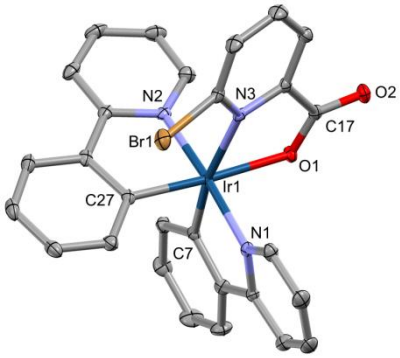

Figure 2. Crystal structure of **4**. Thermal ellipsoids are displayed at 50 % probability, hydrogen atoms and solvent molecules removed for clarity.

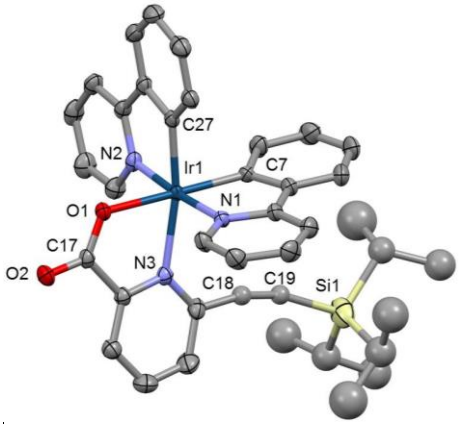

Figure 3. Crystal structure of **8**. Thermal ellipsoids are displayed at 50 % probability, hydrogen atoms, disorder and solvent molecules removed for clarity.

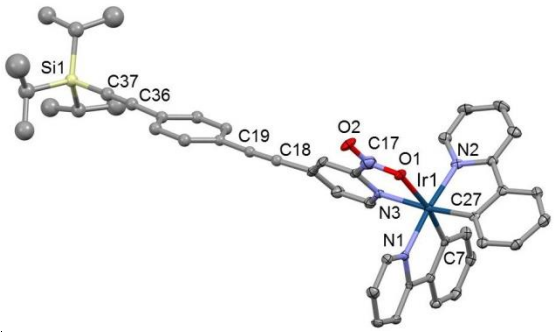

Figure 4. Crystal structure of **9**. Thermal ellipsoids are displayed at 50 % probability, hydrogen atoms, disorder and solvent molecules removed for clarity.

Computational

A brief investigation was performed using DFT calculations to study the electronic structures of complexes **1**–**13**. Initial geometries for the complexes were based on the crystallographic structures of complexes **2**–**6**, **8**, **11** and **12**. The highest-occupied-molecular-orbital (HOMO) for each of the complexes exclusively consisted of iridium and the phenyl group of phenylpyridine, with negligible contributions from either the *pic* or its substituents. As a result, the energy level of this orbital varied less than 0.08 eV for all of the complexes. The lowest-unoccupied-molecular-orbital (LUMO) showed significant variation between the complexes. The LUMO of the bromo-substituted complexes (**1**–**4**) was >90% *pic* in character

with negligible contribution from the bromine in any of the positional isomers. The energy level of the LUMO was *ca*. -2.3 eV for complexes **1**–**4** and **10**. The ethynyl-Tips-substituted complexes (**5**–**8** and **11**) showed a pic-dominated orbital extending onto the alkyne π-orbitals with a 7% (complex **5**) to 16% (complex **6**). It is noted that the LUMO orbital energies of the complexes **6** and **7** are *ca*. 0.2 eV lower than complexes **5** and **8**, suggesting a small effect arising from positional differences. The extended complexes containing the -C≡C-C_6H_4-C≡C-Tips moiety, **9**, **10** and **13** showed an significantly increased degree of localisation on the alkynyl arene in the LUMO with up to 40% contribution from the R group (-C≡C-C_6H_4-C≡C-Tips). As a result, the LUMO energy level for each of these complexes was lowered to -2.64 – -2.60 eV (see Figure 5).

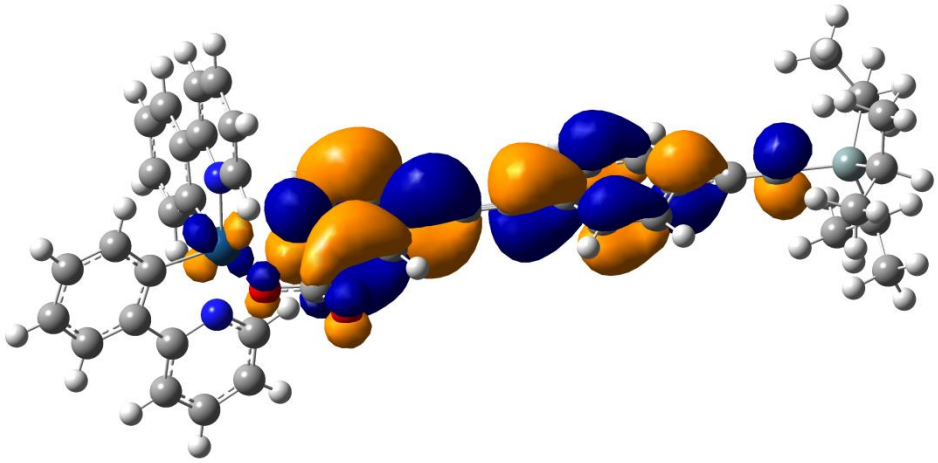

Figure 5. LUMO orbital diagram for complex **9**.

Electrochemistry

Cyclic voltammograms were recorded for all of the complexes in 0.1 M $TBAPF_6$ in dichloromethane and referenced against ferrocene (i.e., $E_{½}$ $FeCp_2$ / $[FeCp_2]^+$ = 0.00 V). Each of the iridium complexes (**1–13**) displayed a single reversible oxidation wave, primarily attributed to the Ir(III)/Ir(IV) couple (see Table 1). Reduction waves were not observed within the solvents electrochemical window.

The bromo-substituted complexes (**1**–**4** and **11**) displayed a small difference with respect to positional substitution, with the highest oxidation potential occurring for complex **4** (E_{ox} = 0.56 V) while the lowest was complex **1**(E_{ox} = 0.51V), which could be attributed to the distortion about the metal centre induced by the steric hindrance of the bromine. Complex **3** also showed a higher oxidation potential, indicating that the substitution about the 5 position had a significant electron-withdrawing effect, more so than any other position. When substituted with 2,4-diphenylpyridine was used in place of 2-phenylpyridine, no effect was observed e.g. complex **2** E_{ox} = 0.53 V while complex **11** E_{ox} = 0.53 V. This is attributed to the localisation at the HOMO of the complex is dominated by the iridium and phenylate group of the ppy ligand and the iridium and as a result modifications made to the pyridine of the ppy ligand had a negligible effect on the oxidation potential of the complex. Substituting the bromo group of the *pic* with an alkyne (complexes **5**-**10** and **12**-**13**) resulted in a small change in oxidation potentials for all of the complexes e.g. complex **2** E_{ox} = 0.53V while complex **9** E_{ox} = 0.51V. The lack of impact on the oxidation potentials is consistent with the computational models which show the pic is most significantly involved in the LUMO and as a result has a limited effect on the oxidation potentials of the molecules.

Photophysical properties

Each of the complexes displayed the characteristic absorption bands assigned as ^{3}MLCT in the range 400–500 nm, with only slight variations in the $\pi \rightarrow \pi^*$ observed for the bromo complexes (**1**–**4** and **11)** and -C≡C-Tips substituted complex (**5**–**8** and **12**). However, for the -C≡C-C_6H_4-C≡C-Tips substituted complexes (**9**, **10** and **13**), showed broadened bands below 400 nm owing to the enhancement of the charge transfer transition between the iridium-ppy and the substituted *pic*, confirmed by the TD-DFT calculations. The absorption of complex **10** was red-shifted *ca.* 20 nm (415 cm^{-1}) compared to complex **9**, suggesting that

there was greater electronic coupling with the 5 position rather than the 4 position of the picolinate.

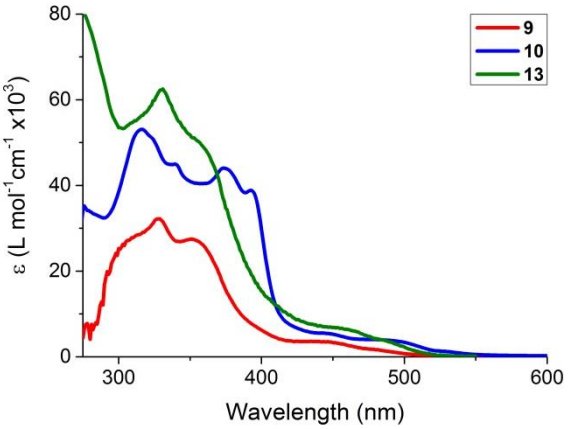

Figure 6. Electronic absorbance spectra of **9**, **10** and **13** recorded in CH_2Cl_2.

Each of the complexes displayed a single featureless emission peak attributed to it being MLCT in nature, supported by the short pure radiative lifetimes (0.74-4.10 µS). Complex **4**'s peak had a negligible intensity suggesting that the geometric distortion caused by the bromide in the 6 position of the pic significantly destabilises the triplet energy state. Complexes **1** and **2** emitted at 611 and 614 nm and complexes **3** and **4** emitted at 589 nm, showing no distinct correlation between the orientations of the bromines about the pic. However, for the -C≡C-Tips substituted complexes, a trend became more significant. Complexes **6** (λ_{emis} = 616 nm) and **7** (λ_{emis} = 636 nm) were notably red-shifted compared to complex **5** (λ_{emis} = 582 nm) and **8** (λ_{emis} = 590 nm), showing the substitutions about the 4 and 5 positions of the pic have the greatest impact on the optical behaviour of the complexes. This was further exaggerated with the -C≡C-C_6H_4-C≡C-Tips substituted complexes (**9**, **10** and **13**), in which the emissions were further red-shifted to 648 nm (complex **10**) and 631 nm (complex **9**) respectively. This was attributed to the increased conjugation red-shifting emissions.

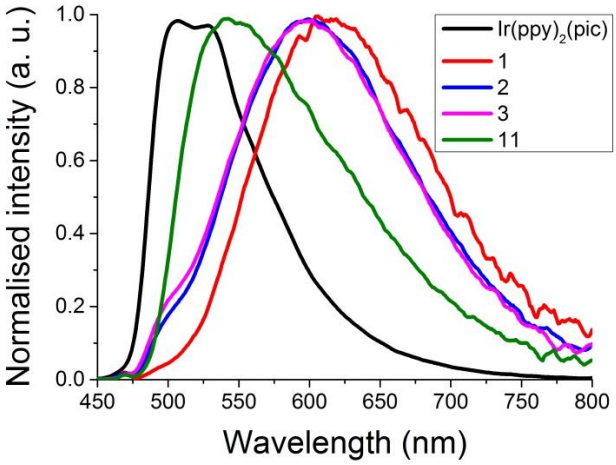

Figure 7. Normalised emission spectra of $Ir(ppy)_2(pic)$, **1**, **2**, **3** and **11** recorded in CH_2Cl_2 excited at 410 nm.

The radiative rate coefficient (k_r) determined for the complexes **1**-**6** and **8**-**13** ranged from 2.44-6.31×10^5 s^{-1} typical for $Ir(ppy)_2(pic)$ complexes and **7** having a higher value of 13.5×10^5 s^{-1},[41] while all of the complexes had non-radiative rate constant (k_{nr}) in the range of 32-542×10^5 s^{-1} significantly higher than that of than that of the parent molecule $Ir(ppy)_2(pic)$ (where k_{nr} = 19.17×10^5 s^{-1}) resulting in low PLQY values, this is attributed to the significant charge transfer to the pic ligand. In addition to the charge transfer the bromo complexes (**1**-**4**) have higher k_{nr} values than that of their -C≡C-Tips complexes (**5**-**8**) due to the heavy atom effect of the bromine, although this difference becomes less significant for the available -C≡C-C_6H_4-C≡C-Tips substituted complexes (**9** and **10**) due to the additional modes for rotation around the free-rotator of the alkyne substituent. The replacement of ppy with Phppy had a negligible effect on either k_r or k_{nr} due to the phenyl groups limited contribution to either the HOMO or LUMO of the complexes.

Table 1. Electrochemical data, emission wavelength, PLQY, lifetimes for the iridium complexes.

Complex	$E_{½}$(ox)	Absorption (ε, 10^4 $Lmol^{-1}cm^{-1}$)	$\lambda_{Emission}$ (nm)	Lifetime (τ, μs)	PLQY (Φ)	T_1 (eV)	k_r (10^5 s^{-1})	k_{nr} (10^5 s^{-1})	Pure radiative lifetime ($\tau_{0,\ \mu s}$)
$Ir(ppy)_2(pic)$[42]	0.51		505	0.514	0.147		2.86	19.17	2.98
1	0.51	263(4.93), 397(0.56)	614	0.038	0.010	2.40	2.63	261	3.80
2	0.53	262(4.82), 397	611	0.039	0.017	2.48	4.36	252	2.29
3	0.55	261(2.99), 396,435	593	0.072	0.040	2.55	5.56	133	1.80
4	0.56	262(5.10), 395(0.64)	589 *	-	-	2.59	-	-	-
5	0.50	266(5.71), 398(0.47)	582	0.058	0.030	2.57	5.17	167	1.93
6	0.50	268(5.65), 329, 430	616	0.155	0.070	2.33	4.52	60	2.21
7	0.52	268(6.40), 352, 400	636	0.065	0.088	2.34	13.5	140	0.74
8	0.50	261(5.48), 398, 440	590	0.278	0.010	2.50	3.60	32	2.78
9	0.51	329(3.35), 352, 435	648	0.111	0.036	2.27	6.31	83	1.59
10	0.51	266(5.3), 289(4.49), 324(4.43), 343(3.91), 396, 438	631	0.041	0.010	2.38	2.44	241	4.10
11	0.53	262(6.79), 271(6.75), 337(2.85), 413	541	0.088	0.036	2.96	4.43	109	2.26
12	0.53	272(8.32), 340(3.17)	622	0.170	0.079	2.35	4.65	542	2.15
13	0.52	272(8.18), 330(6.31)	644	0.118	0.068	2.27	5.76	79	1.74

*low emission

The radiative k_r and non-radiative k_{nr} values in neat film were calculated according to the equations:

$k_r = \Phi/\tau$ and $k_{nr} = (1 - \Phi)/\tau$, from the quantum yields Φ and the lifetime τ values.

Conclusion

Thirteen new bis(2-phenylpyridine)(picolinate)iridium(IV) complexes were synthesised by initially reacting the respective brominated picolinic acid with the corresponding bis(2-phenylpyridine)iridium to produce complexes **1**-**4**. These complexes were reacted with the respective alkyne under Sonogashira conditions to yield the alkyne-substituted complexes. Based on the differences observed in the emission spectra of the complexes, the 4 and 5 positions had the greatest red-shifting effect and therefore have the strongest electronic coupling of all the positions.

ASSOCIATED CONTENT

Supporting Information.

Crystallographic data for compounds **2**-**6** and **8**-**11**. NMR spectra, selected bond parameters and Cartesian coordinates for computational models are given in supporting information.

Notes

The authors declare no competing financial interest.

Acknowledgements

RJD gratefully acknowledge the EPSRC (EP/K007548/1) for funding this work.

Corresponding Authors

***Email: Ross Davidson (Ross.Davidson@Durham.ac.uk) Andrew Beeby (Andrew.Beeby@Durham.ac.uk).

References

1. Yang, C.-H.; Cheng, Y.-M.; Chi, Y.; Hsu, C.-J.; Fang, F.-C.; Wong, K.-T.; Chou, P.-T.; Chang, C.-H.; Tsai, M.-H.; Wu, C.-C., *Angew. Chem. Int. Ed.* **2007,** *46*, 2418-2421.

2. Tsuboyama, A.; Iwawaki, H.; Furugori, M.; Mukaide, T.; Kamatani, J.; Igawa, S.; Moriyama, T.; Miura, S.; Takiguchi, T.; Okada, S.; Hoshino, M.; Ueno, K., *J. Am. Chem. Soc.* **2003,** *125*, 12971-12979.

3. Kozhevnikov, V. N.; Zheng, Y.; Clough, M.; Al-Attar, H. A.; Griffiths, G. C.; Abdullah, K.; Raisys, S.; Jankus, V.; Bryce, M. R.; Monkman, A. P., *Chem. Mater.* **2013,** *25*, 2352-2358.

4. Qian, M.; Zhang, R.; Hao, J.; Zhang, W.; Zhang, Q.; Wang, J.; Tao, Y.; Chen, S.; Fang, J.; Huang, W., *Adv. Mater.* **2015,** *27*, 3546-3552.

5. Gennari, M.; Légalité, F.; Zhang, L.; Pellegrin, Y.; Blart, E.; Fortage, J.; Brown, A. M.; Deronzier, A.; Collomb, M.-N.; Boujtita, M.; Jacquemin, D.; Hammarström, L.; Odobel, F., *J. Phys. Chem. Lett.* **2014,** *5*, 2254-2258.

6. Fleetham, T. B.; Wang, Z.; Li, J., *Inorg. Chem.* **2013,** *52*, 7338-7343.

7. Dragonetti, C.; Valore, A.; Colombo, A.; Righetto, S.; Trifiletti, V., *Inorg. Chim. Acta.* **2012,** *388*, 163-167.

8. Lee, W.; Kwon, T.-H.; Kwon, J.; Kim, J.-y.; Lee, C.; Hong, J.-I., *New J. Chem.* **2011,** *35*, 2557-2563.

9. Chen, F.-F.; Bian, Z.-Q.; Lou, B.; Ma, E.; Liu, Z.-W.; Nie, D.-B.; Chen, Z.-Q.; Bian, J.; Chen, Z.-N.; Huang, C.-H., *Dalton Trans.* **2008**, 5577-5583.

10. Zhang, L.-Y.; Hou, Y.-J.; Pan, M.; Chen, L.; Zhu, Y.-X.; Yin, S.-Y.; Shao, G.; Su, C.-Y., *Dalton Trans.* **2015,** *44*, 15212-15219.

11. Chen, F.-F.; Wei, H.-B.; Bian, Z.-Q.; Liu, Z.-W.; Ma, E.; Chen, Z.-N.; Huang, C.-H., *Organometallics* **2014,** *33*, 3275-3282.

12. Li, L.; Zhang, S.; Xu, L.; Chen, Z.-N.; Luo, J., *J. Mater. Chem. C* **2014,** *2*, 1698-1703.

13. Edkins, R. M.; Sykes, D.; Beeby, A.; Ward, M. D., *Chem. Comm.* **2012,** *48*, 9977-9979.

14. Jones, J. E.; Jenkins, R. L.; Hicks, R. S.; Hallett, A. J.; Pope, S. J. A., *Dalton Trans.* **2012,** *41*, 10372-10381.

15. Chen, F.; Jiang, W.; Lou, B.; Bian, Z.; Huang, C., *Sci. China Ser. B* **2009,** *52*, 1808-1813.

16. Jana, A.; Crowston, B. J.; Shewring, J. R.; McKenzie, L. K.; Bryant, H. E.; Botchway, S. W.; Ward, A. D.; Amoroso, A. J.; Baggaley, E.; Ward, M. D., *Inorg. Chem.* **2016,** *55*, 5623-5633.

17. Lv, W.; Yang, T.; Yu, Q.; Zhao, Q.; Zhang, K. Y.; Liang, H.; Liu, S.; Li, F.; Huang, W., *Adv. Sci.* **2015,** *2*, n/a-n/a.

18. Forster, T., *Farad. Discuss.* **1959,** *27*, 7-17.

19. Dexter, D. L., *J. Chem. Phys.* **1953,** *21*, 836-850.

20. Zhou, Y.; Gao, H.; Wang, X.; Qi, H., *Inorg. Chem.* **2015,** *54*, 1446-1453.

21. Beydoun, K.; Zaarour, M.; Williams, J. A. G.; Roisnel, T.; Dorcet, V.; Planchat, A.; Boucekkine, A.; Jacquemin, D.; Doucet, H.; Guerchais, V., *Inorg. Chem.* **2013,** *52*, 12416-12428.

22. Fischer, L. H.; Stich, M. I. J.; Wolfbeis, O. S.; Tian, N.; Holder, E.; Schäferling, M., *Chem. Eur. J.* **2009,** *15*, 10857-10863.

23. Tian, N.; Thiessen, A.; Schiewek, R.; Schmitz, O. J.; Hertel, D.; Meerholz, K.; Holder, E., *J. Org. Chem.* **2009,** *74*, 2718-2725.

24. Huang, K.; Wu, H.; Shi, M.; Li, F.; Yi, T.; Huang, C., *Chem. Comm.* **2009**, 1243-1245.

25. Li, B.-L.; Wu, L.; He, Y.-M.; Fan, Q.-H., *Dalton Trans.* **2007**, 2048-2057.

26. Munoz-Rodriguez, R.; Bunuel, E.; Fuentes, N.; Williams, J. A. G.; Cardenas, D. J., *Dalton Trans.* **2015,** *44*, 8394-8405.

27. Spaenig, F.; Olivier, J.-H.; Prusakova, V.; Retailleau, P.; Ziessel, R.; Castellano, F. N., *Inorg. Chem.* **2011,** *50*, 10859-10871.

28. Tart, N. M.; Sykes, D.; Sazanovich, I.; Tidmarsh, I. S.; Ward, M. D., *Photochem. Photobiol. Sci.* **2010,** *9*, 886-889.

29. Sykes, D.; Parker, S. C.; Sazanovich, I. V.; Stephenson, A.; Weinstein, J. A.; Ward, M. D., *Inorg. Chem.* **2013,** *52*, 10500-10511.

30. Rausch, A. F.; Thompson, M. E.; Yersin, H., *J. Phys. Chem. A* **2009,** *113*, 5927-5932.

31. Baranoff, E.; Curchod, B. F. E., *Dalton Trans.* **2015,** *44*, 8318-8329.

32. Baranoff, E.; Jung, I.; Scopelliti, R.; Solari, E.; Gratzel, M.; Nazeeruddin, M. K., *Dalton Trans.* **2011,** *40*, 6860-6867.

33. Matt, B.; Moussa, J.; Chamoreau, L.-M.; Afonso, C.; Proust, A.; Amouri, H.; Izzet, G., *Organometallics* **2012,** *31*, 35-38.

34. Matt, B.; Xiang, X.; Kaledin, A. L.; Han, N.; Moussa, J.; Amouri, H.; Alves, S.; Hill, C. L.; Lian, T.; Musaev, D. G.; Izzet, G.; Proust, A., *Chem. Sci.* **2013,** *4*, 1737-1745.

35. Matt, B.; Fize, J.; Moussa, J.; Amouri, H.; Pereira, A.; Artero, V.; Izzet, G.; Proust, A., *Energy. Environ. Sci.* **2013,** *6*, 1504-1508.

36. Giridhar, T.; Cho, W.; Park, J.; Park, J.-S.; Gal, Y.-S.; Kang, S.; Lee, J. Y.; Jin, S.-H., *J. Mater. Chem. C* **2013,** *1*, 2368-2378.

37. Park, H. J.; Choi, H. J.; Seo, H. W.; Hyun, M. H.; Yoon, U. C., *J. Photopolym. Sci. Tec.* **2012,** *25*, 171-174.

38. Zhou, Y.; Li, W.; Liu, Y.; Zeng, L.; Su, W.; Zhou, M., *Dalton Trans.* **2012,** *41*, 9373-9381.

39. Sun, H.; Yang, L.; Yang, H.; Liu, S.; Xu, W.; Liu, X.; Tu, Z.; Su, H.; Zhao, Q.; Huang, W., *RSC Adv.* **2013,** *3*, 8766-8776.

40. Lian, P.; Wei, H.; Zheng, C.; Nie, Y.; Bian, J.; Bian, Z.; Huang, C., *Dalton Trans.* **2011,** *40*, 5476-5482.

41. Baranoff, E.; Curchod, B. F. E.; Monti, F.; Steimer, F.; Accorsi, G.; Tavernelli, I.; Rothlisberger, U.; Scopelliti, R.; Grätzel, M.; Nazeeruddin, M. K., *Inorg. Chem.* **2012,** *51*, 799-811.

42. Xu, M.; Zhou, R.; Wang, G.; Xiao, Q.; Du, W.; Che, G., *Inorg. Chim. Acta.* **2008,** *361*, 2407-2412.

43. Lowry, M. S.; Hudson, W. R.; Pascal, R. A.; Bernhard, S., *J. Am. Chem. Soc.* **2004,** *126*, 14129-14135.

44. Chen, Z.; Grumstrup, E. M.; Gilligan, A. T.; Papanikolas, J. M.; Schanze, K. S., *J. Phys. Chem. B* **2014,** *118*, 372-378.

45. Sheldrick, G., *Acta Crystallogr., Sect. A* **2008,** *64*, 112-122.

46. Dolomanov, O. V.; Bourhis, L. J.; Gildea, R. J.; Howard, J. A. K.; Puschmann, H., *J. Appl. Crystallogr.* **2009,** *42*, 339-341.

47. M. J. Frisch; G. W. Trucks; H. B. Schlegel; G. E. Scuseria; M. A. Robb; J. R. Cheeseman; G. Scalmani; V. Barone; B. Mennucci; G. A. Petersson; H. Nakatsuji; M. Caricato; X. Li; H. P. Hratchian; A. F. Izmaylov; J. Bloino; G. Zheng; J. L. Sonnenberg; M. Hada; M. Ehara; K. Toyota; R. Fukuda; J. Hasegawa; M. Ishida; T. Nakajima; Y. Honda; O. Kitao; H. Nakai; T. Vreven; J. A. Montgomery, J., J. E. Peralta, F. Ogliaro, M. Bearpark, J. J. Heyd, E. Brothers, K. N. Kudin, V. N. Staroverov, R. Kobayashi, J. Normand, K. Raghavachari, A. Rendell, J. C. Burant, S. S. Iyengar, J. Tomasi, M. Cossi, N. Rega, J. M. Millam, M. Klene, J. E. Knox, J. B. Cross, V. Bakken, C. Adamo, J. Jaramillo, R. Gomperts, R. E. Stratmann, O. Yazyev, A. J. Austin, R. Cammi, C. Pomelli, J. W. Ochterski, R. L.

Martin, K. Morokuma, V. G. Zakrzewski, G. A. Voth, P. Salvador, J. J. Dannenberg, S. Dapprich, A. D. Daniels, Ö. Farkas, J. B. Foresman, J. V. Ortiz, J. Cioslowski, and D. J. Fox. *Gaussian 09*, A.1; Gaussian, Inc: Wallingford CT, 2009.

48. Dennington, R.; Keith, T.; Millam, J. *GaussView*, Version 5; Semichem Inc.: Shawnee Mission KS, 2009.

49. O'Boyle, N. M.; Tenderholt, A. L.; Langner, K. M., *J. Comput. Chem.* **2008,** *29*, 839-845.

TABLE OF CONTENTS SYNOPSIS

Using a simple and versatile route for modifying picolinate ligands coordinated to iridium the luminescent behaviour as well as the reactivity of these complexes was examined, showing a dependence on the substitution position about the picolinate ring.

TABLE OF CONTENTS/ABSTRACTS GRAPHIC